Development of a Bearing Test Bench to Investigate Root Causes of Bearing Current Damages

Silvan Scheuermann
Institute of Electrical Engineering (ETI)
Karlsruhe Institue of Technology (KIT)
Karlsruhe, Germany
silvan.scheuermann@kit.edu

Prof. Dr.- Ing. Martin Doppelbauer
Institute of Electrical Engineering (ETI)
Karlsruhe Institue of Technology (KIT)
Karlsruhe, Germany
martin.doppelbauer@kit.edu

Dr. Björn Hagemann
Delta Bruchsal Office
Delta Electronics (Netherlands) B.V.
Bruchsal, Germany
bjoern.hagemann@deltaww.com

Dr. Antoine Jarosz
Delta Bruchsal Office
Delta Electronics (Netherlands) B.V.
Bruchsal, Germany
ajarosz@deltaww.com

Jürgen Kett
Delta Bruchsal Office
Delta Electronics (Netherlands) B.V.
Bruchsal, Germany
juergen.kett@deltaww.com

Johannes Stoß
Institute of Electrical Engineering (ETI)
Karlsruhe Institue of Technology (KIT)
Karlsruhe, Germany
johannes.stoss@kit.edu

***Abstract*— The present paper describes a novel approach of an experimental setup for a bearing test bench to measure the electric impedance of rolling bearings. In this examination, the developed test bench is put in operation and different lubrication types are investigated regarding the bearings' capacitance and its variation. Further, the adapted theory from literature is compared to the results of the bearing capacity measurements. This first study reveals many additional influencing parameters, which must be addressed to reduce discrepancies and to understand the phenomena of electric damage of rolling bearings in traction applications.**

Keywords*— *Electric Machines, Traction Motors, Ball bearings, Parasitic Effects, Failure analysis, Measurement

I. Introduction

Today's electric machines in automotive applications and other traction drives are mainly fed by variable-speed inverter systems. Square-wave pulses of fast-switching inverters with SiC or GaN technology, with steep and high voltage edges can cause bearing currents via the parasitic motor capacitances, which lead to bearing failures. The electrical capacitance of rolling bearings has been investigated in order to characterize the film thickness of the elastohydrodynamic contact between the rolling elements, e.g. [1-3]. Further research was worked out to investigate the occurrence of bearing currents and erosive effects in such contacts. While running a motor, capacitances in the bearings between the outer and inner raceways create a voltage divider proportional to the common-mode voltage, that occurs at the motors' terminal [4,5]. Possible breakdowns of the capacitance and discharges in the bearings' lubrication can cause a meltdown of the raceways' material or lead to the vaporization of the raceways and lubricants. Damage and a reduction in the motor's lifetime is the consequence, which is indicated by a pitted surface or corrugated patterns on the raceways (Figs. 1, 2) [4, 6].

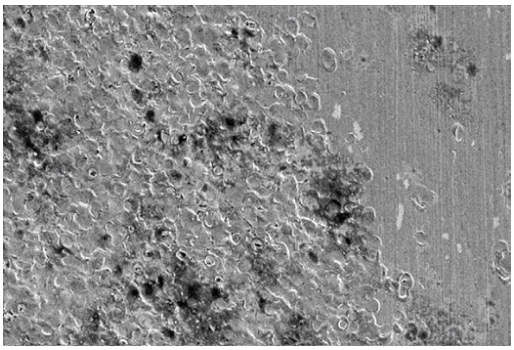

Fig. 1: Pittings on a bearings' raceway [3]

Fig. 2: Corrugated patterns at the raceway

II. Fundamentals

In literature, three types of bearing currents are common. The Electric Discharge Machining (EDM) currents are the consequence of breakdown effects between the two raceways in bearings. Circulating and rotor-to-ground currents besides, are strongly influenced by the common-mode voltage. In the special field of work, the capacitive voltage divider, described by the Bearing Voltage Ratio (BVR) in (1) represents the ratio between the bearing voltage U_b and the common mode voltage U_CM at the motors' terminal.

$$BVR = \frac{U_\mathrm{b}}{U_\mathrm{CM}} = \frac{C_\mathrm{wr}}{C_\mathrm{b,DE} + C_\mathrm{wr} + C_\mathrm{sr} + C_\mathrm{b,NDE}} \tag{1}$$

The constituent parts of the BVR are the winding-to-rotor capacitance C_wr, the stator-to-rotor capacitance C_sr, but also the bearings' capacitances of the drive- ($C_\mathrm{b,DE}$) and non-drive-end ($C_\mathrm{b,NDE}$). A common approach, to characterize rolling bearings under elasto-hydrodynamic (EHD) conditions, is to characterize each rolling element as a single capacitor. The Hertzian contact area A_Hertz forms an analogy of a plate capacitor between the rolling element and the raceways. The thickness of the lubricating film h_0, which is the distance between these figurative plates has the highest influence on the magnitude of the capacity. Further the permittivity ε_r of the lubrication changes due to a variation in pressure or temperature [7]. For example in [8], the Hertzian capacitance of the bearings is calculated by:

$$C_\mathrm{Hertz} = k_\mathrm{Hertz}\varepsilon_0\varepsilon_\mathrm{r}\frac{A_\mathrm{Hertz}}{h_0} \tag{2}$$

Since not only the contact area A_Hertz itself contributes to the Hertzian capacitance, but also the undeflected surrounding

area must be taken into account. Therefore [8] et al. introduced an empirical correction factor k_{Hertz}, which is based on measurements and calculations and varies between 1.1 and 4 [8]. The parameters in (2) depend on factors like pressure, temperature, contact force, curvature radius, combined Young's Modulus E', hydrodynamic speed, or viscosity η_0 [9]. As described in [9], the capacitance of a ball bearing is also influenced by many running conditions as consequence of a change in temperature, speed, load, and lubrication properties. E.g., an increase in speed lowers the capacitance due to a rebound in lubrication film height. An increase in radial load rises the capacity because the Hertzian contact area increases due to a larger rolling element deformation and a decrease in lubrication thickness. Furthermore, starvation effects at very high speeds or a rise in temperature lead to higher capacitances because of a decrease in viscosity and film thickness. In summary, the Hertzian contact area is the main influence for the capacitance which decreases with higher film thickness [9].

III. Analytcal Determination of the Ball Bearings' Capacity

A. Theory

In the following, to determine the relevant quantities for the bearings' capacitances, such as the lubricant film thickness and the Hertzian contact area, theoretical relations are depicted. According to Hamrock and Dowson [9] the lubricant film thickness in each rolling contact can be calculated by (3).

$$h_0 = 2.69 \cdot r_{\mathrm{x}} \cdot (1 - 0.61 \cdot e^{-0.73 \cdot k}) \cdot \bar{U}_{\mathrm{r}}^{0.67} \cdot (\alpha \cdot E')^{0.53} \cdot \bar{W}^{-0.067} \quad (3)$$

As mentioned in the previous chapter, the lubrication film thickness h_0 depends not only on the load or pressure of each rolling element, but also on geometric quantities like the curvature radius r and material properties. E.g., the combined Young's Modulus E' influences the calculation. In context of (3) and (4), $\bar{U}_r$ describes the dimensionless velocity and $\bar{W}$ the dimensionless load of one rolling element.

$$\bar{U}_r = \frac{\eta_0 \cdot U_{\mathrm{r}}}{E' \cdot r_{\mathrm{x}}} \quad (4)$$

$$\bar{W} = \frac{W_{\max}}{E' \cdot r_{\mathrm{x}}^2} \quad (5)$$

$$E' = \frac{E}{1 - \nu^2} \quad (6)$$

α describes the viscosity-pressure coefficient of the lubricant and the combined Youngs' Modulus E' is defined by (6) with the Youngs' Modulus E and Poisson number ν. Equation (3) combines the ratio of the main radii of curvature r_{x} and r_{y} to the ellipticity factor k. This geometric quantity is used to estimate the relationship between the large and small half-axis of an ellipse. The maximum load of one rolling element $W_{\max}$ is estimable by Equation 7, with the whole load of the bearing W_{L} and the number of rolling elements N_{WK}. By means of the angle velocity ω and the geometric data of a bearing, the rolling velocity U_{r} can be calculated. Lastly, (7) allows to estimate the Hertz' contact area using the two main axis a and b.

$$A_{\mathrm{Hertz}} = \pi \cdot a \cdot b = \pi \cdot \left(\frac{6 \cdot \hat{E} \cdot W_{\max} \cdot r_{\mathrm{eq}}}{\pi \cdot k \cdot E'}\right)^{\frac{1}{3}} \cdot \left(\frac{6 \cdot k^2 \cdot \hat{E} \cdot W_{\max} \cdot r_{\mathrm{eq}}}{\pi \cdot E'}\right)^{\frac{1}{3}} \quad (7)$$

The factor r_{eq} describes the equivalent main radius of the curvature. $\hat{E}$ is another geometrical estimation factor, which was defined in [5]. Equation (8) defines another correction factor which was introduced in [5], that describes the influence of starvation effects.

$$k_{\mathrm{s}} = e^{-\frac{6 \cdot \omega}{300 \cdot \pi}} + 0.1 \quad (8)$$

Finally, the whole bearing's capacitance is calculated as the combination of the inner-raceway capacity C_{i} and the outer-ring capacity C_{o} by (9) as in [9].

$$C_{\mathrm{b}} = \frac{\sum_{N_{\mathrm{WK}}} C_{\mathrm{i},k} \cdot \sum_{N_{\mathrm{WK}}} C_{\mathrm{o},k}}{k_{\mathrm{s}} \cdot (\sum_{N_{\mathrm{WK}}} C_{\mathrm{i},k} + \sum_{N_{\mathrm{WK}}} C_{\mathrm{o},k})} \quad (9)$$

B. Determination of the Capacitances of the Bearings SKF 6011 and SKF 61813

In the following, the capacitance of the two ball bearing types SKF 6011 [10] and SKF 61813 [11] are calculated analytically as well as determined by a Finite Element (FE) analysis. The two single-row deep groove ball bearings were chosen because of their versatility. Further, they have low friction, and are optimized for low noise and low vibration, which enables high rotational speeds. The benefits include that they withstand radial and axial loads in both directions, are easy to mount, and require less maintenance than many other bearing types. These are some reasons, why they are also used in many traction applications [10, 11]. The properties and specifications are shown in Table (1), based on the information in [10-16].

TABLE I. Properties and Specifications of Ball Bearings

Property	***SKF 6011***	***SKF 61813***
Number of balls N_{WK}	13	24
Radius of inner race curvature r_{in}	31.07 mm	34.72 mm
Radius of inner race r_{i}	5.37 mm	2.848 mm
Radius of balls r_{WK}	5.16 mm	2.778 mm
E-modulus E	208000 MPa [9]	
Poisson number ϑ	0.3 [9]	
Load of each bearing $W_{\max}$	7 N	
Viscosity-pressure coefficient α	2.3e-8 N^{-1} [9]	

The load of each bearing $W_{\max}$ remains from the weight force of the shaft of the test bench. The viscosity-pressure coefficient α is a standard value, extracted from [12]. The material data of the bearings' races and balls, which are made of 100Cr6 or SUJ2 steel are retrieved from [12]. As described in Section I, [8] introduced an empirical correction factor k_{Hertz}, which is defined as a constant of 3.5. The analytical capacity calculation of the fixed bearing SKF 6011 varies

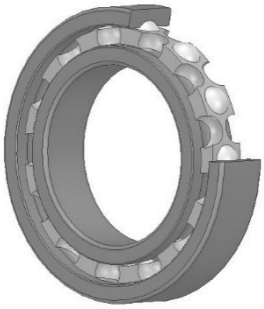

Fig. 3: 3D Model of bearing SKF 6011

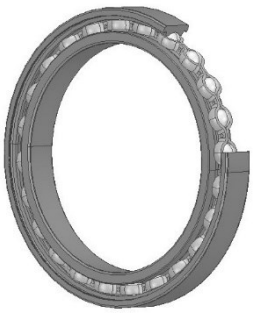

Fig. 4: 3D Model of bearing SKF 61813

between $C_{\mathrm{FB,ana}} = 181.31\ pF$ and $106.38\ pF$. The floating bearing's capacity (SKF 61813) varies between $C_{\mathrm{FLB,ana}} = 240\ pF$ and $120\ pF$. The calculation is very dependent on the shaft speed and correction factors. The exact values are presented in Fig. 6 in dependence of the speed. The determination of the bearings' capacity by a 3D FE-analysis obtains a value of $C_{\mathrm{FB,FEM}} = 129.86\ pF$, respectively $C_{\mathrm{FLB,FEM}} = 264.27\ pF$ in stillstand. The 3D models are shown in Figs. 3 and 4. The deviation from the analytically determined values by formulas strengthens the theory to represent the capacitance of loaded bearings, while the FE analysis calculates the capacity of unloaded bearings with an even distributed radial clearance over the whole circumference besides a consideration of ideal undeformed balls. Since a 3D analysis was conducted, it must be mentioned, that the number of cells for the meshing could have influenced the accuracy of the results. Nevertheless, the FE analysis has had the aim to determine a benchmark value for the capacitance only, and this objective was achieved well. Without proof here, a sensitivity analysis of the bearing in other FE simulations shows, that halving the number of balls will result in almost halving the magnitude of the bearings' capacity, while a non-consideration of the bearings' cage will result in a reduction of the capacity by approx. $20\ pF$. Further must be mentioned, that the loads and the different speeds in real bearings' applications are not implemented in the FE-simulations. Multi-body or similar simulations can be used to improve the results, which exceeds the scope of this study.

IV. Bearing Test Bench

Fig. 5 shows the novel approach of a bearing test bench for traction applications, which was used to perform all

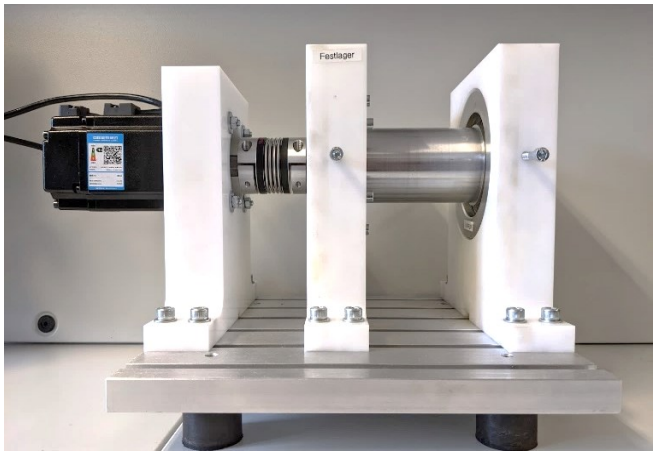

Fig. 5: Novel approach of the bearing test bench

measurements. It consists of a drive motor, which is connected to the main shaft by an interchangeable coupling. The above-presented bearings, SKF 6011 and SKF 61813 are the load carrying bearings of this main shaft. The servo motor Delta ECMA-C10807RS is fed by an in-house developed ETI-System-on-Chip inverter, which allows not only the control of the system, but also can capture other precious data like torque, speed, currents, or external loads and temperature [17, 18]. The coupling is implemented by a R+W BKH/15/59/8/19 metal bellows coupling to measure the voltage signal of the shaft, induced by the common mode voltage of the drive unit which can be replaced to e.g. a R+W EKH/20/B/8/19 elastomer coupling. The elastomer coupling is necessary to separate all noisy voltage signals from the impedance analyzer. The motor, as well as the shaft, are mounted on brackets, made of non-conducting polyoxymethylene (POM) to measure the two bearings separately from each other and without noise from the structure's environment. To ensure a defined operability of the system, which should mirror a traction application, a preload washer provides an axial preload. For the contact between the bearings and the connecting terminals of the impedance analyzer, two conducting bolts are threaded through the POM racks, which

TABLE II. Properties and Specifications of the Lubricants

Lubricant	*Category*	*Density*	*Kinematic viscosity*
Würth HHS 2000	Oil	$0.742\ g\ cm^{-3}$	$> 20\ mm^2\ s^{-1}$
Würth HHS Fluid	Viscous grease	$0.773\ g\ cm^{-3}$	$> 25\ mm^2\ s^{-1}$
Würth HHS Lube	Grease	$0.78\ g\ cm^{-3}$	-
Shell S6 ATF D971	Oil	$0.822\ g\ cm^{-3}$	$18\ mm^2\ s^{-1}$

touch the outer rings of each bearing. This makes it possible to measure the bearings' capacitances in a series connection or separately as series connection between the bearing and shaft. Two transparent plates with a sealing ring serve to hold all grease and oil inside or around the bearings, but also to prevent external dirt. For the impedance measurement, a Keysight E4990A impedance analyzer in the measurement range between $10\ kHz$ and $5\ MHz$ was used, and afterward, the measured capacitances C_{meas} were averaged over the constant measurement range. For the first investigations of the bearings' capacitances, three different sprayable lubricants have been investigated. Besides, an automatic transmission fluid (ATF) for automotive applications was used in this study. The details and further specifications can be found in the respective data sheets [13-16]. To ensure the comparability of the measurements between different lubricants, which are either grease, liquid grease or automatic transmission fluid, they were sprayed in the same amount of approx. $4\ ml$ into the bearings. Afterwards, the test bench was accelerated to $1000\ rpm$ and the speed was held for one minute to distribute the lubricants equally, before the measurement routine started.

V. Results

In Fig. 6, the measurement results of the capacitance versus speed for both bearing types, SKF 6011 and SKF 61813 with no additional radial load are presented. Generally,

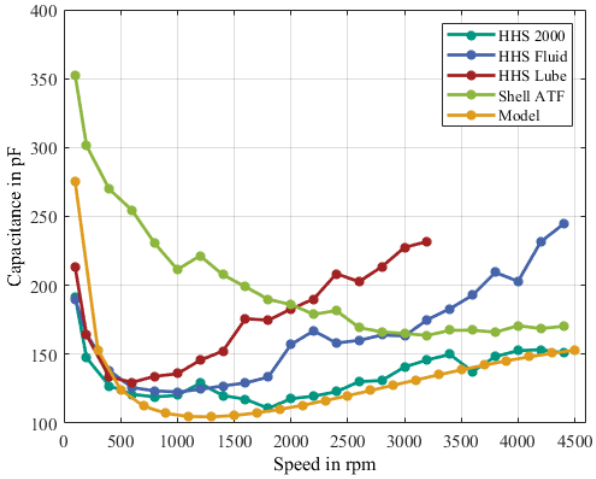

Fig. 6a: Capacitance over speed of the SKF 6011 bearing

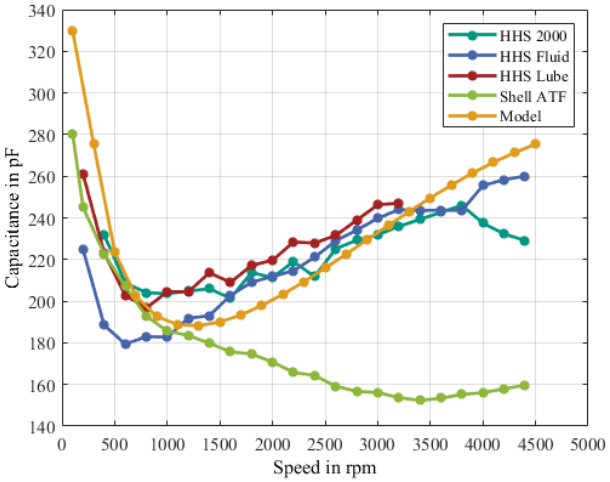

Fig. 6b: Capacitance over speed of the SKF 61813 bearing

for both bearings, in the case of the sprayable lubricants, the plots show initially a decrease in the capacitance while the shaft speed increases. This can be explained by the flow of lubrication into the ball-ring contact with increasing rolling speed so that a lubricant film builds up, becomes thicker and the capacity thus becomes smaller [6]. A further increase in shaft speed forces the lubricant out of the contact zone. Due to the viscosity of the lubricant and the high rolling frequency, it can no longer flow back into the contact zone fast enough, which is called the "starvation effect". The consequence is a thin lubrication film because the contact zone "starves" of lubrication. That's the reason for an increasing capacitance [9]. The study for the SKF 6011 bearing in combination with the Würth HHS Lube lubricant reveals this effect clearly. Above 3200 min^{-1}, no capacitance, but a resistive impedance instead, can be measured. This indicates that the viscosity of this lubricant is too high so that not enough lubrication is in the contact zone after acceleration and a separating lubricating film can no longer be formed. This reasoning explains furthermore the different slopes of the measured capacitances.

Consequently, due to the low viscosity of the HHS 2000, the oil can flow back easily in the contact zone, which forms a uniform lubrication film height already at lower speeds and a flatter increase in capacitance. The comparison of the two plots for the bearings indicates that a capacitive behavior for all lubricants can be measured above 100 min^{-1} for the 6011 bearing, while the SKF 61813 bearing needs at least a speed of 200 min^{-1}, which means higher speeds are required to build up a separating lubricating film. All curves for the floating bearing are on a higher level, which can be explained by the higher number of balls N_{WK}. This effect has been seen also in the FE-analysis. Further can be observed, that the capacitances for the fixed bearing SKF 6011 diverge widely, while the curves for the floating bearing remain closer together. This is also explainable by the number of balls N_{WK}, their smaller ball diameter but also because of the lower radial clearance. That concludes that a variation in lubrication type is not the dominant influence on the capacitance. The curves for the very low viscous Shell ATF show a different behavior than the curves of the sprayable lubricants. The capacitance of the fixed bearing SKF 6011 in combination with the ATF decreases quickly with an increasing shaft speed but then remains on an almost constant plateau. It is very noticeable, that the capacitance is at a higher level. This phenomenon is explainable by the very low oil film height and the low viscosity. Both contribute to the fact that all oil can flow out of the relevant Hertz' surface area without effort. Already at low shaft speeds, the lubricant film height is at a minimal level and remains constant over the whole measurements' speed range. The measurement curve of the floating bearing SKF 61813 indicates a similar behavior.

The comparison of the measurements to the analytical model reveals that a model can describe the capacitive behavior of one bearing quite well, independent of the bearing type. It must be disclosed that many correction factors are needed to determine the capacity of one bearing, in combination with a specific lubricant approximately. Furthermore, every combination needs its individual correction factors to provide a benchmark number of the capacitance for a loaded bearing (see also [4 – 6, 8, 9]).

VI. Discussion

This preliminary study shows, that a general determination of a bearing's capacity, neither by analytical geometry-based formulas nor by measurements is easily possible. Well defined running and measurement conditions, as well as detailed information about the bearing size, radial and axial clearance, the lubricants' physical properties and its behavior in a changing environment are very important. Not only the viscosity or density of the lubricant is an essential factor, also the temperature and the temperature increase when the test bench is in operation contribute to offsets in the measurement curves. The changing properties of the lubrication, e.g. viscosity or permittivity makes it hard to predict the behavior in dynamic operation in early motor design phases. The starvation effect makes it further inevitable to develop a correction factor. In literature, all correction factors are empirical and were derived from and fitted to measurement curves. An analytical approach to model the effects, which are considered by such correction factors correctly does not exist yet. Moreover, the established analytical model was originally built to provide a benchmark number of the capacitance for a loaded bearing. In this study the bearings were only loaded by the gravity force of the test bench's components.

VII. Summary and Outlook

In this research, a new method to determine a bearing's capacity is demonstrated. The test bench is designed to investigate and to understand parasitic properties, which can occur in electric motors. After a superficial presentation of the common analytical determination of the bearings' capacity,

the developed test bench was explained, in what follows the measurement results of this test bench. In the study, different lubricants are investigated and compared to an analytical model for the characterization of the bearings' behavior. In summary, it can be concluded, that only with help of many correction factors, the capacitance can be estimated approximately, especially the qualitative progression of the curves can be predicted. The study reveals that one formula cannot cover all cases, grease, and oil lubrication, combined. It must be underlined, that this paper focuses on the development of a new test bench to determine the bearings' capacitances. Besides, the examination reveals the dependency of the capacitance on many more factors than reported in literature, which must be investigated in further work.

The test bench will be extended by a feature to apply radial forces, measured by a load cell. Further axial loads will be applied by a preload washer with a well-known force displacement characteristic. Another extension will be the temperature measurement of the bearings and the lubrication, which was perceived as an important factor for the bearings' capacitive behavior. Further, a new measurement setup connected to the bearing test bench will provide the excitation of an external current in the already known magnitude of the EDM currents acquired from literature, e.g. [8, 9], to provoke a damage.

The ultimate goal is a determination of the bearings' capacitances, and their modeling in operation so that predictions for the bearings' lifetime are possible. This will help to assess the character of the electric motors and the destructive power of potential bearing currents regarding the motors' lifetime and operationality already in early motor development phases.

REFERENCES

[1] A. W. Crook, "The Lubrication of Rollers II. Film Thickness with Relation to Viscosity and Speed," Philosophical Transactions of the Royal Society A: Mathematical, Physical and Engineering Sciences, vol. 254, no. 1040, pp. 223–236, 1961.

[2] P. Brüser, "Untersuchungen über die elastohydrodynamische Schmierfilmdicke bei elliptischen Hertzschen Kontaktflächen," Dissertation, Fakultät für Maschinenbau und Elektrotechnik, Technische Universtität Braunschweig, Braunschweig, 1972.

[3] A. Dyson, H. Naylor, and A. R. Wilson, "The Measurement of Oil-Film Thickness in Elastohydrodynamic Contacts," Proceedings of the Institution of Mechanical Engineers, Conference Proceedings, vol. 180, no. 2, pp. 119–134, 1965.

[4] Bader, N., Furtmann, A., Tischmacher, H., & Poll, G. "Capacitances and lubricant film thicknesses of grease and oil lubricated bearings." STLE Annual Meeting & Exhibition. 2017.

[5] P. Han, G. Heins, D. Patterson, M. Thiele, & D.M. Ionel (2021). Modeling of Bearing Voltage in Electric Machines Based on Electromagnetic FEA and Measured Bearing Capacitance. IEEE Transactions on Industry Applications, 57, 4765-4775.

[6] A. Furtmann, "Elektrisches Verhalten von Maschinenelementen im Antriebsstrang," Dissertation, Wilhelm Leibniz Universität Hannover, Hannover, 2017.

[7] Bondi A. Physical chemistry of lubricating oils. New York: Book Division, Reinhold Pub. Corp; 1951.

[8] Gemeinder Y, Schuster M, Radnai B, Sauer B, Binder A. Calculation and validation of a bearing impedance model for ball bearings and the influence on EDM-currents. In: 2014 International Conference on electrical machines (ICEM). IEEE; 2014. p. 1804–10.

[9] E. C. Wittek, "Charakterisierung des Schmierungszustandes im Rillenkugellager mit dem kapazitiven Messverfahren", Gottfried Wilhelm Leibniz Universität Hannover, Hannover, 2017.

[10] SKF. https://www.skf.com/uk/products/rolling-bearings/ball-bearings/deep-groove-ball-bearings/productid-6011 (last visit: 27.11.2022)

[11] SKF. https://www.skf.com/uk/products/rolling-bearings/ball-bearings/deep-groove-ball-bearings/productid-61813 (last visit: 27.11.2022)

[12] IBC-Wälzlager GmbH, Wälzlagerwerkstoffe. Adress: https://www.ibc-waelzlager.com/files/IBC_Waelzlagerwerkstoffe.pdf. (last visit: 27.11.2022)

[13] Würth. HHS 2000 Safety Data Sheet. https://pim.wurth.ca/Technical/SDS_893.106.pdf (last visit: 28.11.2022)

[14] Würth. HHS Technical Data in overview. https://www.klickparts.com/out/media/124266.pdf (last visit: 28.11.2022)

[15] Würth. HHS Lube Safety Data Sheet. https://shop.wohlfeil.de/media/pdf/28/c9/39/Sicherheitsdatenblatt_HHSLube.pdf (last visit: 28.11.2022)

[16] Shell. Spirax S6 ATF D971. https://www.shell-livedocs.com/data/published/en/e18a9d59-95f6-4f7e-b29e-aa598d9fbbcd.pdf (last visit: 28.11.2022)

[17] B. Schmitz-Rode et al., "A modular signal processing platform for grid and motor control, HIL and PHIL applications," 2022 International Power Electronics Conference (IPEC-Himeji 2022- ECCE Asia), Himeji, Japan, 2022, pp. 1817-1824

[18] J. Stoß et. al, "Design guideline for PCB integrated, high bandwidth, current slope sensing based on a planar Rogowski coil," 2021 23rd European Conference on Power Electronics and Applications (EPE'21 ECCE Europe), Ghent, Belgium, 2021, pp. P.1-P.10